Available online at www.sciencedirect.com

ScienceDirect

Procedia Structural Integrity 47 (2023) 820–825

Structural Integrity Procedia

www.elsevier.com/locate/procedia

27th International Conference on Fracture and Structural Integrity (IGF27)

Integral Macrostructural Characteristics Of Carbon Composite Based On Microtomographic Data

A.M. Ignatova[a]1, M.V. Bannikov[a], Yu.V. Bayandin[a], A.N. Balakhnin[a],

K.E. Kuper[b], O.B. Naimark [a]

[a] *Institute of Continuous Media Mechanics of the Ural Branch of Russian Academy of Science (ICMM UB RAS), 1, Academika Koroleva st., Perm, 614013, Russian Federation*

[b]*Budker Institute of Nuclear Physics of Siberian Branch Russian Academy of Sciences (BINP SB RAS), 11, Acad. Lavrentieva Pr., Novosibirsk, 630090, Russian Federation*

Abstract

Methodology is developed to compare integral structural characteristics of carbon composite material (CCM) under static and cyclic loads using microtomography. Bayesian Gaussian Mixture-based threshold segmentation and cluster analysis detected small and large pores associated with mechanical loads. Under cyclic loads, pore size increases and closely located pores clusterization is observed affecting the strength of specimens. Pore orientation distribution and coherence are uncorrelated, and a sample without load has three clusters of pores classified by orientation distribution. Pore clustering and ordering change differently under quasi-static and cyclic loads, but orientation distribution remains unchanged. The findings improve understanding of CCM behavior under load and aid in developing strength prediction models.

Keywords: Type

1. Introduction

Carbon-carbon composites (CCMs) are materials composed of carbon fibers bound together by a carbon matrix. These materials have high strength, stiffness, resistance to high temperatures, and abrasion resistance. They are among the most promising materials in civil engineering, including aviation and energy industries. Numerous studies

* Corresponding author.
E-mail address: aditya@ft.uns.ac.id (A.R.P.); ristiyanto.adiputra@brin.go.id (R.A.)

10.1016/j.prostr.2023.07.037

on different carbon composites (Cai Y. et al. (2017), Li Z. et al. (2018), Lu W. et al. (2019), Sutradhar A. and Pal S. K. (2017) and Wang L. et al. (2019)) have shown that their macrostructural and morphological characteristics are closely related to mechanical properties and failure. Analysis of the modal properties of acoustic signals by non-destructive MAE (Modal Acoustic Emission) method found the following damage features in carbon composites: delamination, formation of cracks in the matrix, and fiber rupture (Jiang P. et al. (2022) and Nebe M. et al. (2021)).

Despite the obvious interconnections, most studies focusing on the mechanical behavior of carbon composites do not investigate their structural characteristics or morphology. It is expected that the presence of damage, microcracks, and other heterogeneities such as pores can lead to a decrease in their strength and durability. The study by Kastner J. et al. (2013) notes that there is a direct correlation between porosity and mechanical properties, such as compressive strength, shear strength, and elasticity modulus. It was established by Birt E.A. and Smith R.A. (2004) that the interlaminar shear strength decreases by 7% for every 1% of porosity.

Research reviewing allowed the conclusion that morphometric parameters of pores in the structure of carbon composites are morphologically altered during loading. The behavior of pores during loading becomes one of the main factors determining the mechanical parameters of the material. Understanding the behavior of pores in the material during loading is crucial for predicting the operational resource of carbon composites, which can be achieved using non-destructive testing methods.

There are numerous non-destructive testing methods available to determine the porosity parameters of composites (Weissenböck J. et al. (2017), Plank B. et al. (2015) and Mehdikhani M. Et al. (2019)), including promising among them is X-ray-based tomography. This method allows for data to be obtained on the size and volume of the structure elements in three dimensions. Radiographic images are interpreted into a volumetric dataset using computational methods. In each position of the resulting dataset, a gray value is calculated that corresponds to the spatial X-ray attenuation coefficient. The spatial X-ray attenuation coefficient is a measure that describes how much X-ray radiation is attenuated when passing through a specific material type at a certain thickness. When processing composite material data, each position in the image corresponds to a specific component of the macrostructure and has its unique spatial attenuation coefficient. Calculating gray values based on this coefficient allows the creation of an image where the material density at each point is displayed. Currently, the determination of the real and accurate porosity values of carbon composites using tomography is still under investigation. However, pores have a sufficiently large and developed internal surface area, so the accuracy of determining the porosity parameters depends heavily on the method of analyzing images obtained from tomography.

Ng H-F. (2006), Xu H. et al. (2019) and Ren H. et al. (2021) made the conclusion, that segmentation methods are the most effective tool for analyzing images of carbon composites in tomography. There are four main types of segmentation. Threshold segmentation is a method based on defining the boundary between an object and the background based on setting a threshold value of pixel intensity, belonging to the object, and below which it belongs to the matrix.

Regional segmentation is a method based on identifying regions with similar brightness or texture values. It allows for the identification of areas that do not correspond to the matrix or object but have similar characteristics to other areas.

Model-based methods are those that use pre-defined models to determine objects in the image. They allow for the identification of objects that correspond to the specified model.

Supervised learning-based methods are those used to train algorithms on many annotated images. These methods typically allow for higher segmentation accuracy than model-based methods.

It is shown by Schuller J. and Oster R. (2006), that the segmentation method based on a global threshold value for analyzing tomography data provides the most accurate estimate of porosity with a high degree of repeatability and correspondence to results obtained using ultrasound porosity estimation.

The aim of this study is to develop a method for comparative evaluation of integral macrostructural characteristics of fiber-reinforced composite materials under static and cyclic loading based on microtomography data analysis of material porosity parameters.

2. Materials and methods

Unidirectional carbon fabric with an epoxy matrix CW200-TW2/2 was studied comparing tomography results of the material's macrostructure before and after both quasi-static and cyclic loading. The samples were used as sheet blanks with the size 250x25x4 mm and 6 mm diameter hole in the center as a stress concentrator. Cylindrical samples with a diameter of Ø2 mm and a height of 4 mm were cut out (using a hollow diamond drill) from the sample from the areas located on different distances from stress concetrator, their positions are indicated in Fig. 1.

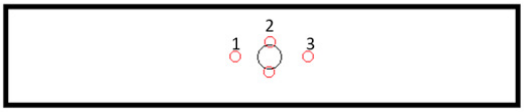

Figure 1. Scheme of sample cutting: (1) - zone with low influence of load on the structure; (2) - zone in the stress concentrator area; (3) - zone along the load axis.

Quasi-static loading was done using the Shimadzu AGX-plus electro-mechanical universal testing machine, with samples loaded at a constant speed of 1 mm per minute up to 85% of the ultimate stress value. Cyclic loading was performed on a Biss-00-100 servo-hydraulic universal testing machine with a maximum load amplitude of 50-80% of the maximum destructive load, cycle asymmetry coefficient R of 0.1, and testing frequency of 10 Hz, until reaching 500,000 load cycles. A synchrotron X-ray radiation source from a wiggler on the VEPP-3 charged particle accelerator was used for tomography, with a spatial resolution of 1 μm for the short wavelength range (5-30 keV). Porosity matrices were analyzed using ImageJ-FiJi and the OrientationJ plugin, with statistical processing using a clustering analysis method based on Bayesian Gaussian Mixture using Python.

3. Results and their discussions

Fig. 2 displays diagrams representing cluster analysis based on the study of pore volume and surface area in the CCM samples. The analysis revealed that all samples had a high positive covariance between pore surface area and volume, and cluster differences were mostly due to differences in surface area. Two clusters, small and large pores, were identified based on pore volume and surface area for all samples, but each sample had unique cluster characteristics (see Table 1).

Under mechanical and cyclic loading, pores in the CCM samples increase in size with the increase in force, and new damages occur in parallel with the growth of already existing pores. Under cyclic loading, pores located close to each other are more likely to increase in size with origin of large voids.

Cluster analysis indicates that there is a negative correlation between the factor of dispersion and the distance between the closest pores in all samples, implying that these two characteristics are independent. Differences between the clusters are determined by the distance between the pores, while the value of the factor of dispersion varies more for individual samples than for clusters. The average value of the factor of dispersion for samples not influenced by deformation loads is 2.87 μm^{-1}, while for samples subjected to quasi-static and cyclic loads, the values range from 1.83 μm^{-1} to 2.02 μm^{-1}. The obtained data supports previous observations that the largest pore size was characteristic of samples along the loading axis under quasi-static and cyclic loads, and that smaller pores have a higher factor of dispersion.

For all four samples, pores are divided into three clusters based on their distance: closely spaced pores, pores located at intermediate distances, and far-spaced pores (Table 2). Most pores are located far apart from each other, with the highest proportion of closely spaced pores present in the unstrained sample at 18.06%. The proportion of far-spaced pores increases with applied load, with the highest proportion of pores located far apart from each other being characteristic of the sample obtained from the stress concentrator zone under quasi-static testing at 52.88%. Pore proximity is a factor determining the strength of CCM samples. The diagrams in Fig. 3 show the results of cluster analysis for pores based on their orientation distribution and coherence. There is a low covariance between the orientation distribution and coherence for the examined specimens, indicating they are independent characteristics.

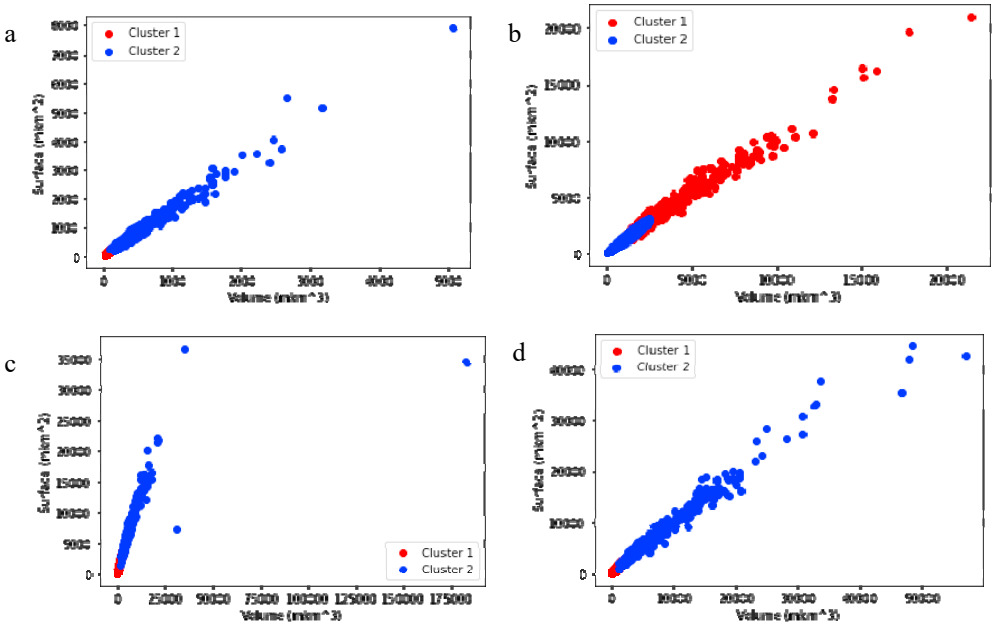

Figure 2. Diagrams characterizing the results of cluster analysis by volume and surface area for samples: (a) without loading; (b) after quasi-static loading in the stress concentrator area; (c) after quasi-static loading along the loading axis; (d) after cyclic loading along the loading axis.

Table 1. Results of cluster analysis for pores based on their volume and surface area.

Pore characteristics	Sample type							
	unloaded state		after quasistatic loading in the stress concentrator region state		after quasistatic loading along the loading axis state		after cyclic loading along the loading axis	
	Cluster 1	Cluster 2	Cluster 1	Cluster 2	Cluster 1	Cluster 2	Cluster 1	Cluster 2
Average volume (V), μm^3	93.90	413.05	970.10	3688.60	1124.33	6866.76	997.02	6354.24
Average surface area (S), μm^2	192.10	727.72	1238.07	4105.60	1443.89	7059.00	1284.39	6669.47
Fraction of the total volume, %	80.18	19.82	80.97	19.03	91.46	8.54	84.04	15.96

Table 2. Results of cluster analysis of pores based on the factor of dispersion and distance between the nearest pores.

Pore characteristics	Sample type											
	unloaded state			after quasistatic loading in the stress concentrator region state			after quasistatic loading along the loading axis state			after cyclic loading along the loading axis		
	Cluster 1	Cluster 2	Cluster 3	Cluster 1	Cluster 2	Cluster 3	Cluster 1	Cluster 2	Cluster 3	Cluster 1	Cluster 2	Cluster 3
Dispersion factor (S/V), μm^{-1}	2.87	2.86	2.87	2.01	2.01	2.03	1.85	1.81	1.83	1.80	1.85	1.86
Distance between pores, μm	35.23	376.17	141.28	103.81	333.08	14.13	374.21	23.99	122.73	15.47	106.47	353.91
Fraction of the total volume, %	18.06	47.12	34.82	34.37	52.88	12.75	48.96	16.75	34.29	14.92	33.5	51.58

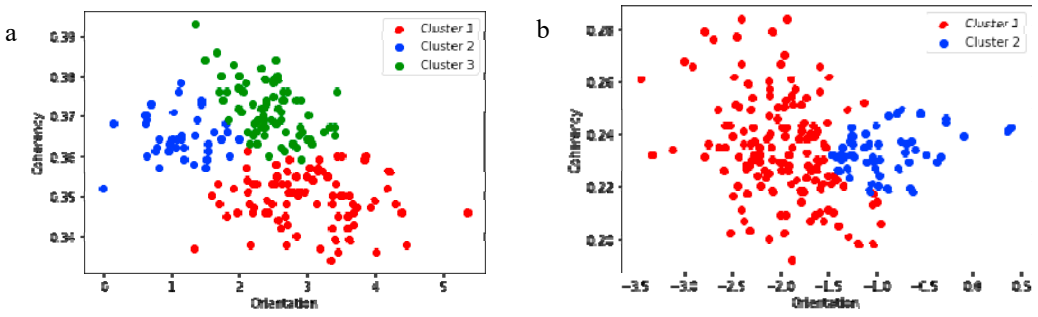

Figure 3. Diagrams characterizing the results of cluster analysis of pores based on their orientation distribution and coherence for the samples: (a) without loading; (b) after cyclic loading along the loading axis.

For samples under quasi-static loads, pore clustering wasn't observed. Ordered pores tended to decrease without changing their orientation distribution, which may be due to the origin of small pores into larger defects. The sample from the stress concentrator area had an average orientation distribution value of 2.47° with an average coherence of 0.24, while the sample located on the loading axis had an average orientation distribution value of -2.26° (with a negative value indicating a possible sample orientation artifact) and an average coherence of 0.25. For a sample under cyclic loading, pores are divided into two clusters based on their orientation distribution. The first cluster has a mean orientation distribution of -1.97° and a coherence of 0.23, representing 67.85% of the pores. The second cluster has a mean orientation distribution of -1.20° and a coherence of 0.23, representing 32.15% of the pores. Under cyclic loading, the ordering of pores tends to remain unchanged, while their orientation distribution shifts towards a more horizontal orientation, possibly due to pore coalescence caused by material stratification.

4. Conclusion

Methodology is proposed for the comparative assessment of integral structural characteristics of CCM under static and cyclic loading based on microtomography data, using threshold segmentation and cluster analysis based on Bayesian Gaussian Mixture. The study revealed the presence of small and large pores in CCM, the volume and surface area of which are correlated with each other and linked to mechanical loads. The pore size increases under loading, especially under cyclic loading. Closely located pores merge during loading, so the proportion of closely located pores is an important factor in determining the strength of the samples. The orientation distribution and coherence are not related to each other, and the sample without loading has three clusters of pores divided according to the orientation distribution. Under quasi-static loading, pore clustering and pore ordering decrease, but the orientation distribution remains unchanged. Under cyclic loading, pores are divided into two clusters determined by the orientation distribution, and the orientation becomes more horizontal. The ordering of pores is also observed to be preserved under cyclic loading.

Acknowledgements

The research was conducted with the support of the Russian Science Foundation (Project No. 21-79-30041).

References

Birt E A and Smith R A. A review of NDE methods for porosity measurement in fibrereinforced polymer composites. Insight 2004; 46(11): 681-686.

Cai, Y., Li, Y., & Li, M. (2017). A hybrid method for automatic segmentation of voids in X-ray computed tomography images of carbon fiber reinforced polymer composites. Composites Science and Technology, 139, 103-112. https://doi.org/10.1016/j.compscitech.2016.12.005

Ignatova A.M., Balakhnin A.N., Bannikov M.V., Kuper K.E., Nikitiuk A.S., Naimark O.B. Technique for obtaining an integral characteristic of the structure of a loaded composite material based on microtomographic research data // Procedia Structural Integrity. - 2022. - V.41. - P.550-556 https://doi.org/10.1016/j.prostr.2022.05.063.

Jiang, P.; Liu, X.; Li, W.; Guo, F.; Hong, C.; Liu, Y.; Yang, C. Damage Characterization of Carbon Fiber Composite Pressure Vessels Based on Modal Acoustic Emission. Materials 2022, 15, 4783. https://doi.org/10.3390/ma15144783

Kastner, J., Plank, B., Salaberger, D., & Sekelja, J. (2013). Defect and porosity determination of fibre reinforced polymers by X-ray computed tomography. Composites Science and Technology, 85, 74-81. doi: 10.1016/j.compscitech.2013.06.003.

Li, Z., Fan, H., Zhang, D., Liu, S., & Wang, G. (2018). Mechanical behavior and damage evolution of 3D-woven C/SiC composites under tensile loading: In-situ observation and digital image correlation. Composites Science and Technology, 167, 305-313. https://doi.org/10.1016/j.compscitech.2018.09.021

Lu, W., Chen, Q., Zhang, Y., & Xu, C. (2019). Microscopic analysis of a composite material with different fiber architectures based on digital image correlation and computed tomography. Composites Part B: Engineering, 167, 421-429. https://doi.org/10.1016/j.compositesb.2019.03.013

Mehdikhani, M., Straumit, I., Gorbatikh, L., & Lomov, S. V. (2019). A dataset of void characteristics in multidirectional carbon fiber/epoxy composite laminates, obtained using X-ray micro-computed tomography. Data in Brief, 27, 104686. doi: 10.1016/j.dib.2019.104686

Nebe, M.; Soriano, A.; Braun, C.; Middendorf, P.; Walther, F. Analysis on the mechanical response of composite pressure vessels during internal pressure loading: FE modeling and experimental correlation. Compos. Part B Eng. 2021, 212, 108550.

Ng H-F. Automatic thresholding for defect detection. Pattern recognition letters 2006; 27: 1644-1649.

Plank, B., Gusenbauer, C., Senck, S., Hoeller, H., & Kastner, J. (2015). Porosity determination in CFRP by means of X-ray computed tomography methods. Materials Testing, 57(5), 365-370. doi: 10.3139/120.110721

Ren, H., Huang, G., Li, L., Zhang, J., & Wang, D. (2021). Automated segmentation and quantification of carbon fiber in composite materials using convolutional neural network. Journal of Reinforced Plastics and Composites, 40(8-9), 356-368.

Schuller J and Oster R. Classification of porosity by ultrasonic in carbon fibre helicopter

structures based on micro computed tomography, Proceedings European conference on nondestructive testing, Berlin, Germany, 25.–29. September 2006

Sutradhar, A., & Pal, S. K. (2017). Quantitative microstructural analysis of a carbon fiber reinforced polymer composite using image processing techniques. Journal of Materials Science, 52(14), 8572-8584. https://doi.org/10.1007/s10853-017-1104-4

Wang, L., Cai, W., Li, X., Liu, B., & Zhou, Y. (2019). Quantitative characterization of the local stiffness of a fiber-reinforced composite using micro-computed tomography and image-based modeling. Composites Science and Technology, 171, 77-86. https://doi.org/10.1016/j.compscitech.2018.12.001

Weissenböck, J., Senck, S., Plank, B., Heinzl, C., & Kastner, J. (2017). Porosity evaluation of carbon fiber-reinforced polymers with porosity analyzer. Polymer Testing, 57, 154-161. doi: 10.1016/j.polymertesting.2016.11.017

Xu, H., Wang, Y., Tang, J., & Li, H. (2019). An automatic segmentation method for micro-CT images of carbon fiber composites based on the convolutional neural network. Measurement, 146, 406-416.